HHS Public Access

Author manuscript

Neuroscience. Author manuscript; available in PMC 2019 February 21.

Published in final edited form as:

Neuroscience. 2018 February 21; 372: 225–236. doi:10.1016/j.neuroscience.2017.12.048.

Anti-nociceptive role of CXCL1 in a murine model of peripheral nerve injury-induced neuropathic pain

Ling Cao[1,2,3] and **Jennifer T. Malon**[1,2]

[1]Department of Biomedical Sciences, College of Osteopathic Medicine, Biddeford, ME 04005

[2]Center for Excellence in the Neurosciences, University of New England, Biddeford, ME 04005

[3]Graduate School of Biomedical Sciences and Engineering, University of Maine, Orono, ME 04473

Abstract

Both spinal cord infiltrating CD4+ T lymphocytes and microglial CD40 contribute to the maintenance of neuropathic pain-like behaviors induced by spinal nerve L5 transection (L5Tx), a murine model of neuropathic pain. Here, we sought to investigate the involvement of multiple chemokines in microglial CD40-mediated and CD4+ T lymphocytes-mediated L5Tx-induced sensory hypersensitivity. Spinal cord chemokine expression in CD4 knockout (KO), CD40 KO, and wild type (WT) BALB/c mice was determined at the protein level via multiplex assays and at the RNA level via quantitative real-time PCR. In WT mice, L5Tx induced significant increases in CCL2, CCL3, and CCL5 expression (protein and RNA) up to day 21 post-L5Tx, while CD4 KO mice displayed blunted, predominantly non-significant, responses in these chemokines at protein levels post-L5Tx. L5Tx also induced increased expression of these chemokines in CD40 KO mice; however, the overall protein levels of these chemokines were significantly lower than that in WT mice. Further, L5Tx induced a significant increase in CXCL1 at the protein level and in CXCR2 at RNA level only in CD40 KO mice. Intrathecal administration of CXCL1 in WT mice significantly reduced L5Tx-induced mechanical hypersensitivity. CD40 KO mice also displayed higher levels of Ly6G (neutrophil marker) RNA expression in the lumbar spinal cord post-L5Tx. Altogether, our data suggest that CD4+ T lymphocytes and microglial CD40 mediate their pro-nociceptive effects in part by promoting selected chemokine responses, and more importantly, CXCL1 can play an anti-nociceptive role in peripheral nerve injury induced neuropathic pain, which is possibly mediated by infiltrating neutrophils.

Keywords

Neuropathic pain; Spinal nerve L5 transection; CD4; CD40; Chemokines; CXCL1

Corresponding author: Ling Cao MD PhD, Department of Biomedical Sciences, College of Osteopathic Medicine, University of New England, 11 Hills Beach Road, Biddeford, ME 04005, USA, Tel: 1-207-602-2213, Fax: 1-207-602-5931 lcao@une.edu.

Introduction

Chronic pain affects approximately 100 million adults in the United States, with an estimated annual cost up to $635 billion (Gaskin and Richard, 2012). Neuropathic pain, defined as pain caused by a lesion or disease of the somatosensory system, is one of the most devastating kinds of chronic pain (Jensen et al., 2011). Unfortunately, treatment is still suboptimal. Delineating the mechanisms leading to neuropathic pain is essential to facilitate the development of more effective treatments. There is ample evidence that the development of neuropathic pain is closely related to immune responses. The role of one group of immune molecules, chemokines, has attracted more attention in recent years. Chemokines are a family of small secreted chemoattractant proteins that stimulate the migration and activation of various types of leukocytes (such as T cells, B cells, and monocytes) and play a central role in inflammatory responses. Chemokines have been implicated in various inflammatory diseases in both the peripheral and the central nervous systems (Charo and Ransohoff, 2006, Callewaere et al., 2007), as well as in the development of neuropathic pain (White et al., 2007, Gao and Ji, 2010). For example, reduced sensory hypersensitivity has been observed in CCL2 (monocyte attractant protein -1 (MCP-1)) receptor (CCR2) knockout (KO) mice following sciatic nerve ligation (Abbadie et al., 2003) and in mice treated with CCL2 neutralizing antibodies following spinal nerve ligation (Gao et al., 2009). Similarly, mice either lacking CCL5 (regulated on activation, normal T cell expressed and secreted (RANTES)) or intraperitoneally administered with a selective CCL5 receptor antagonist, Met-RANTES, showed reduced sensory hypersensitivity following partial sciatic nerve ligation (Liou et al., 2012, Liou et al., 2013). Furthermore, our recent study indicated that CCL5 is a key chemokine mediator in CGRP-induced mechanical hypersensitivity following spinal nerve L5 transection (L5Tx) (Malon and Cao, 2016). In addition, CX3CL1 (Fractalkine) /CX3CR1 signaling has also been examined extensively as a critical pathway that facilitates the communication between sensory neurons and resident microglia in the development of neuropathic pain (Zhang et al., 2013, Clark and Malcangio, 2014). Together, these studies highlight the importance of chemokines in the development of neuropathic pain.

Previously, in studying the involvement of adaptive immunity in the development of neuropathic pain, we showed that there is a transient infiltration of CD4+ T cells, predominantly type 1 helper T cells, into the lumbar spinal cord following L5Tx, and CD4+ cell adoptive transfer experiments indicated the contribution of CD4+ T lymphocytes in the maintenance phase of L5Tx-induced mechanical hypersensitivity(Cao and DeLeo, 2008, Draleau et al., 2014). To investigate the potential role of the infiltrating CD4+ T cells within the spinal cord, we examined the role of microglial CD40 (interaction between microglial CD40 and CD40 ligand expressed by activated T cells provides a pathway for the interaction between infiltrating CD4+ T cells and resident microglia) and demonstrated that microglial CD40 also plays a critical role in the maintenance of L5Tx-induced mechanical hypersensitivity (Cao and DeLeo, 2008, Draleau et al., 2014). In addition, our results showed a greater reduction of L5Tx-induced mechanical hypersensitivity in CD40 KO mice and in the CD40 KO-WT chimeric mice (mice that do not have CD40 expression in the central nervous system (CNS)) than in CD4 KO mice, suggesting that microglial CD40

plays a more substantial role in neuropathic pain compared to infiltrating CD4+ T cells. We suspect this is partially due to CD40's greater influence on microglial activation (Cao et al., 2012a), and studying CD40-mediated responses may reveal novel treatment strategies.

In the current study, we sought to further investigate the involvement of chemokines in both the roles of CD4+ T cell-mediated and microglial CD40-mediated mechanisms in the development of neuropathic pain. A multiplex assay and qRT-PCR were used to assess the expression of various chemokines in the lumbar spinal cord following L5Tx in both CD4 KO and CD40 KO mice. Our results pointed to a potential anti-nociceptive effect of CXCL1, which may be due to an increased recruitment of neutrophils in the spinal cord following injury.

Experimental procedures

Animals

Male and female adult wild type (WT) BALB/c mice (7–8 weeks old) were purchased from the Frederick Animal Facility (Frederick, MD) of the Charles River Laboratories (Wilmington, MA). All mice were allowed to habituate to the institutional animal facility for at least one week before experimental use. As previously described in detail (Cao and DeLeo, 2008, Cao et al., 2009), breeding pairs for BALB/c-CD4 KO mice and BALB/c-CD40 KO mice were originally obtained from Dr. William T. Lee of the Wadsworth Center, New York State Department of Health and the Jackson Laboratory (Bar Harbor, ME) respectively, and maintained at the University of New England (UNE) animal facility by breeding respective homozygous KO mice. All mice were group-housed (3–4 per cage) with food and water *ad libitum* and maintained on a 12-h light/dark cycle. The overall ratio between male and female mice within individual genotypes used in each set of experiments was approximately 1:1. All experimental procedures used in this study were approved by the Institutional Animal Care and Use Committee (IACUC) at UNE.

L5Tx surgery and CXCL1 administration

Spinal nerve L5 transection (L5Tx) and sham surgeries were performed on adult mice (8–9 weeks old) following our previously published procedures (Cao and DeLeo, 2008). For experiments that examining the effects of CXCL1 on the development of L5Tx-induced sensory hypersensitivity, mouse recombinant CXCL1 (BioLegend, San Diego, CA, carrier-free and at 200 μg/ml) at 1 ng or 10 ng/5 μl were intrathecally (i.t.) injected daily from days 6 to 13 post-surgery. This time period was chosen based on the expression of CXCL1 in the spinal cord (Figure 1K). i.t. injections were performed according to our previously published procedure (Malon et al., 2011). Mice received vehicle (sterile saline) i.t. injection, and mice that received no i.t. injections were used as controls. On days when behavioral tests were conducted on the same day as an injection, the injection was given after the behavior tests.

Behavioral tests

Both mechanical and heat sensitivities were determined with mice under non-restrained conditions as previously described (Cao et al., 2012b). Briefly, the mechanical sensitivity was determined via the von Frey test following the up-down method (Chaplan et al., 1994)

and the 50% threshold force needed for paw withdrawal was calculated to represent animal's mechanical sensitivity. The heat sensitivity was measured via the Hargreaves test using an IITC thermal plantar analgesia instrument for mice (IITC Life Science, Woodland Hills, CA) and the average paw withdrawal latencies of 3 separate tests (with an interval of at least 10 min) was used to represent animal's heat sensitivity. Mice were baseline tested two to three times before day 0 (the day of surgery) and then repeatedly tested at selected days as indicated up to day 20 post-surgery. When von Frey up-down and Hargreaves tests were performed on the same day, mice were tested with von-Frey test first and then given at least 1 hour to acclimate before the Hargreaves test to avoid potential influence between tests. The person performing the behavioral tests was blinded to the experimental groups.

Chemokine multiplex assay

Chemokine multiplex assay was performed by technicians at the Quansys Biosciences (Logan, UT) with lumbar spinal cord tissue homogenates prepared with tissue lysis buffer containing proteinase inhibitor cocktail (Sigma-Aldrich, St. Louis, MO), as described previously (Malon and Cao, 2016). A total of 8 chemokines were included in the manufacturer's pre-designed multiplex assay: CXCL1 (keratinocyte-derived chemokine, (KC)), CCL1 (T-cell activation protein-3 (TCA-3)), CCL2 (MCP-1), CCL3 (macrophage inflammatory protein-1α (MIP-1α)), CCL5 (RANTES), CCL11 (eotaxin), CCL17 (thymus- and activation-regulated chemokine (TARC)), and CCL22 (macrophage-derived chemokine (MDC)). Tissue levels of chemokines were normalized to the total protein levels of each sample, as determined by BCA assays (ThermoFisher Scientific, Waltham, MA).

RNA isolation and chemokine quantitative real time polymerase chain reaction (qRT-PCR)

At selected days post-surgery, lumbar spinal cords were harvested and immediately frozen on dry ice and stored at −80°C until RNA isolation. The total tissue RNA was isolated with the RNeasy Lipid Tissue kit (QIAGEN, Germantown, MD, USA) following the manufacturer's instructions. cDNA was then synthesized from 1 μg of tissue RNA using the Quanta qScript ™ Supermix (Quanta Bio, Beverly, MA) according to the manufacturer's instruction. qRT-PCR for CXCL1, CCL2, CCL3, CCL5, CXCR2, and Ly6G (Lymphocyte antigen 6 complex, locus G; known to be a marker for neutrophils (Fleming et al., 1993)) were then performed with 0.5 μl of cDNA and the Quanta PerfeCTa™ SYBR Green FastMix ROX (Quanta Bio, Beverly, MA) using the Applied Biosystem StepOnePlus Real-Time PCR System thermal cycler (Applied Biosystems, Grand Island, NY). For CXCL1, CXCR2 and Ly6G, and the corresponding glyceraldehyde 3-phosphate dehydrogenase (GAPDH) control, the PrimeTime primer mixes (summarized in Table-1) was obtained from Integrated DNA Technologies (IDT, Coralville, IA, USA) and qRT-PCR was performed following the suggested protocol by IDT: 95°C for 30 sec followed by 40 cycles of 95°C for 3 sec and 60°C for 30 sec, with fast ramp speed. For CCL2, CCL3, and CCL5, and their corresponding GAPDH control, primer sequences (summarized in Table-1; synthesized by IDT) and PCR protocol: 95°C for 15 min, followed by 40 cycles of 95°C for 15 sec and 60°C for 1 min, were obtained from a previously published study (Christophi et al., 2009). Chemokine expression was determined using the ΔΔCt method with normalization to GAPDH.

Statistical analysis

All statistical analyses were performed using SigmaStat 3.5 (Systat Software, Inc.). Appropriate analysis of variance (ANOVA) with genotype, treatment, and time as main factors were performed followed by Student-Newman-Keuls (SNK) *Post hoc* analysis. Note that due to limited production of KO mice, it was not possible to determine the sex differences in all of the data sets. The results were described in the text when "sex" factor was evaluated. All data are presented as mean ± SEM. $p < 0.05$ was considered as statistically significant.

Results

Lumbar spinal cord chemokine expression post-L5Tx in both CD4 KO and CD40 KO mice

Adult male and female CD4 KO, CD40 KO, and WT BALB/c mice were randomly assigned to either L5Tx or sham groups, as well as individual time groups. At selected times, days 0 (naïve animals), 3, 7, 14, and 21 post-surgery, the lumbar spinal cord from each mouse was harvested and processed for a chemokine multiplex assay performed by technicians at the Quansys Biosciences. Out of the 8 chemokines measured, 4 chemokines, CCL2, CCL3, CCL5, and CXCL1 displayed significant increases in one or more of the mouse genotypes following surgery. Thus data for these 4 chemokines are shown here (in Figure 1, raw data are presented, and in Figure 2, data are presented in percentage change (naïve = 100% within each genotype of mice)). CCL11 displayed a non-statistically significant trend of increase post-L5Tx in both WT and CD40 KO mice (not shown). Our initial Three-way ANOVAs with genotype, surgery type, and time as factors indicated significant differences between genotypes (Figures 1 and 2, Three-way ANOVA, $p_{genotype} < 0.001$ for all, $p_{timexgenotype} < 0.01$ for CCL5 (Figures 1G and 2G), and $p_{timexgenotype} = 0.013$ for CCL2 (Figures 2A)). Therefore, data are presented based on individual genotypes. Since naïve CD40 KO mice expressed much lower levels of these chemokines compared to naïve WT and CD4 KO mice (Figure 1, one-way ANOVA comparing WT, CD40 KO, and CD4 KO naïve groups, $p < 0.05$ for all 4 chemokines), data are also presented as a percent change within each genotype for easy visualization (Figure 2, naïve = 100%; note that the statistical analysis would yield the same results within each genotype regardless if raw data or percentage changes were used as the relationship between the individual values did not change when data were normalized to the corresponding naïve control group). In WT mice, L5Tx induced significant, gradual increases of 3 chemokines: CCL2, CCL3, and CCL5, up to day 21 post-surgery compared to sham controls (Figure 1A and 2A, for CCL2, two-way ANOVA, $p_{time} = 0.027$, $p_{surgery} = 0.005$ and $p_{timexsurgery} = 0.166$; Figure 1D and 2D, for CCL3, two-way ANOVA, $p_{time} < 0.001$, $p_{surgery} = 0.011$ and $p_{timexsurgery} = 0.488$; Figure 1G and 2G, for CCL5, two-way ANOVA, $p_{time} = 0.313$, $p_{surgery} = 0.004$ and $p_{timexsurgery} = 0.178$). In CD40 KO mice, although L5Tx also induced significant increases of CCL2 and CCL5 as in WT mice, and the fold increase for these chemokines were greater in CD40 KO mice than that in WT mice, the overall absolute levels of these chemokines were lower in CD40 KO mice compared to that in WT and CD4 KO mice (Figure 1B and 2B, for CCL2, two-way ANOVA, $p_{time} < 0.001$, $p_{surgery} = 0.018$ and $p_{timexsurgery} = 0.258$; Figure 1E and 2E, for CCL3 two-way ANOVA, $p_{time} = 0.189$, $p_{surgery} = 0.596$ and $p_{timexsurgery} = 0.829$; Figure 1H and 2H, for CCL5, two-way ANOVA, $p_{time} = 0.002$, $p_{surgery} = 0.620$ and

$p_{timexsurgery}$ = 0.544). Further, the differences in CCL2 levels between injured and sham-operated CD40 KO mice were appreciable as that in WT mice, yet the surgery-group differences in CCL5 levels were less remarkable in CD40 KO mice compared to that in WT mice. Contrary to both WT and CD40 KO mice, in CD4 KO mice, the only statistical significances detected were elevations of CCL5 levels at days 14 and 21 post-surgery. However, the differences between injured and sham-operated CD4 KO mice were indistinguishable, suggesting a CD4-mediated suppression of surgery-induced CCL5 production (Figures 1C and 2C, for CCL2, two-way ANOVA, p_{time} = 0.514, $p_{surgery}$ = 0.986 and $p_{timexsurgery}$ = 0.539; Figures 1F and 2F, for CCL3, two-way ANOVA, p_{time} = 0.426, $p_{surgery}$ = 0.427 and $p_{timexsurgery}$ = 0.855; and Figures 1I and 2I, for CCL5, two-way ANOVA, p_{time} = 0.001, $p_{surgery}$ = 0.694 and $p_{timexsurgery}$ = 0.408). Interestingly, L5Tx induced a significant elevation of CXCL1 levels in CD40 KO mice but not in either WT or CD4 KO mice (Figures 1J and 2J, Two-way ANOVA, p_{time} = 0.740, $p_{surgery}$ = 0.101 and $p_{timexsurgery}$ = 0.882; Figures 1K and 2K, Two-way ANOVA, p_{time} = 0.040, $p_{surgery}$ = 0.095 and $p_{timexsurgery}$ = 0.600; Figures 1L and 2L, Two-way ANOVA, p_{time} = 0.200, $p_{surgery}$ = 0.673 and $p_{timexsurgery}$ = 0.590). In addition, although both male and female mice were used, due to the large variability in chemokine levels and limited production of the knockout animals (particularly CD4 KO mice), no firm conclusions regarding sex differences can be concluded at this time (sex-separated data not shown). Nevertheless, it appeared that in WT mice, the L5Tx-induced increase of CCL2, CCL3, and CCL5 peaked around days 7–14 post-surgery in males, while the increases in females were gradual and reached maximal levels at day 21 (the time point of study termination) post-L5Tx.

Further, lumbar spinal cord expression of CCL2, CCL3, CCL5, and CXCL1 were also determined at the RNA level in all three types of mice following L5Tx or sham surgery and compared to RNA levels from day 0 (naïve) samples. At baseline (in naïve mice), CD40 KO mice showed significantly higher levels of CCL2 and CXCL1 compared to WT mice, while no significant differences in CCL3 or CCL5 transcripts were detected between genotypes (Figure 3, one-way ANOVA, for CCL2, $p_{genotype}$ = 0.015; CCL3, $p_{genotype}$ = 0.913, CCL5, $p_{genotype}$ = 0.770; and CXCL1, $p_{genotype}$ = 0.042). Thus, baseline levels of each genotype of mice were considered as 100%, and percentage changes in the transcript levels of these chemokines were further analyzed (Figure 3). As expected, similar to the changes in protein levels described above, initial three-way ANOVA with genotype, surgery type and time as factors indicated significant genotype effects on the changes of these selected chemokines following L5Tx (Figure 4, Three-way ANOVA, for CCL2, $p_{genotype}$ = 0.003; for CCL3, CCL5 and CXCL1, $p_{genotype}$ < 0.001). In WT mice, consistent with the changes at protein levels, L5Tx significantly increased the RNA levels of CCL2, CCL3, and CCL5 compared to sham surgery, with the most notable increase being seen in CCL2 (Figure 4A, for CCL2, two-way ANOVA, p_{time} < 0.001, $p_{surgery}$ < 0.001 and $p_{timexsurgery}$ < 0.001; Figure 4D, for CCL3, two-way ANOVA, p_{time} = 0.189, $p_{surgery}$ < 0.001 and $p_{timexsurgery}$ = 0.192; Figure 4G, for CCL5, two-way ANOVA, p_{time} = 0.039, $p_{surgery}$ = 0.590 and $p_{timexsurgery}$ = 0.476). In CD40 KO mice, changes in CCL2, CCL3, and CCL5 at the transcript level also support the changes of these chemokines observed at the protein level. That is, L5Tx induced significant increases of CCL2, CCL3, and CCL5, with CCL5 showing a greater fold-increase compared to WT mice (Figure 4B, for CCL2, two-way ANOVA, p_{time} < 0.001,

$p_{surgery} < 0.001$ and $p_{timexsurgery} < 0.001$; Figure 4E, for CCL3, two-way ANOVA, $p_{time} = 0.4$, $p_{surgery} = 0.001$ and $p_{timexsurgery} = 0.205$; Figure 4H, for CCL5, two-way ANOVA, $p_{time} < 0.001$, $p_{surgery} < 0.001$ and $p_{timexsurgery} < 0.001$). Contrary to the less remarkable changes observed at the protein level, L5Tx induced significant increases of CCL2 and CCL5 at the transcript level in CD4 KO mice (Figure 4C, for CCL2, two-way ANOVA, $p_{time} = 0.002$, $p_{surgery} = 0.004$ and $p_{timexsurgery} = 0.470$; Figure 4F, for CCL3, two-way ANOVA, $p_{time} = 0.072$, $p_{surgery} = 0.898$ and $p_{timexsurgery} = 0.993$; Figure 4I, for CCL5, two-way ANOVA, $p_{time} < 0.001$, $p_{surgery} = 0.905$ and $p_{timexsurgery} = 0.150$). Finally, unlike that observed at the protein level, changes in CXCL1 at the transcript level were only observed in WT mice and without significant differences between L5Tx and sham surgery groups (Figure 4J, two-way ANOVA, $p_{time} = 0.004$, $p_{surgery} = 0.191$ and $p_{timexsurgery} = 0.477$; Figure 4K, two-way ANOVA, $p_{time} = 0.161$, $p_{surgery} = 0.176$ and $p_{timexsurgery} = 0.773$; and Figure 4L, two-way ANOVA, $p_{time} = 0.039$, $p_{surgery} = 0.870$ and $p_{timexsurgery} = 0.971$).

In addition, as CXCR2 is the corresponding receptor for CXCL1, we also examined the RNA levels of CXCR2 in the lumbar spinal cord in WT, CD40 KO and CD4 KO mice. There is no significant difference in CXCR2 expression between WT, CD40 KO and CD4 KO mice at the basal level. Three-way ANOVA using genotype, time and surgery as factors indicated a significant genotype effects, primarily the differences between CD40 KO mice vs. CD4 KO and WT mice respectively (Figure 5, Three-way ANOVA, $p_{genotype} = 0.023$, $p_{time} = 0.219$ and $p_{timexsurgery} = 0.834$; CD40 KO vs. CD4 KO, $p = 0.019$, CD40 KO vs. WT, $p = 0.090$, and CD4 KO vs. WT, $p = 0.259$). Within each genotype, there is a slight increase in CXCR2 expression following surgery (regardless of L5Tx or sham) in all three types of mice; however, statistical significance was only achieved in CD40 KO mice (Figure 5A, two-way ANOVA, $p_{time} = 0.098$, $p_{surgery} = 0.607$ and $p_{timexsurgery} = 0.280$; Figure 5B, two-way ANOVA, $p_{time} = 0.050$, $p_{surgery} = 0.771$ and $p_{timexsurgery} = 0.654$; and Figure 5C, two-way ANOVA, $p_{time} = 0.160$, $p_{surgery} = 0.917$ and $p_{timexsurgery} = 0.639$). Thus, increased CXCR2 expression could facilitate CXCL1 signaling in CD40 KO mice.

Anti-nociceptive effects of CXCL1 in WT mice

While the reduction of the elevation of and/or the lower absolute levels of CCL2, CCL3, and CCL5 in CD4 KO and CD40 KO mice (Figures 1 and 2) may in part explain the reduced mechanical hypersensitivity following L5Tx observed in both CD4 KO and CD40 KO mice (Cao and DeLeo, 2008, Cao et al., 2009), the unique increase in CXCL1 at the protein level in CD40 KO mice suggests a different role of CXCL1 in L5Tx-induced sensory hypersensitivity. To further investigate the effect of CXCL1 in L5Tx-induced sensory hypersensitivity, i.t. injections of recombinant mouse CXCL1 were administered to WT mice and both mechanical and heat sensitivities were examined up to day 20 following L5Tx. CXCL1 was given daily from day 6 to day 13 post-L5Tx; during the peak increase of CXCL1 observed in CD40 KO mice (Figures 1K and 2K). Mouse body weights were monitored throughout the treatment from before surgery (Day 0) to day 20 post-surgery when the experiment was terminated. Significant interactions between sex and time, and sex and treatment were detected using three-way ANOVA ($p_{sex} < 0.001$, $p_{sexxtime} < 0.001$ and $p_{sexxtreatment} < 0.001$). Thus, further multi-group comparisons were made within each sex. Normal expected body weight changes were observed for individual animals which

included: increases in body weight over time, slight decrease following L5Tx, and slower increase with repeated i.t. injections (not marked on individual graphs to avoid confusion). Multi-group comparisons did indicate significant sex-dependent differences in body weight changes between treatment groups. On days 14 and 17 post-L5Tx, male mice that received the higher dose of CXCL1 (10 ng/5 μl/injection) had significantly lower body weights compared to saline injected mice (Figure 5A, two-way RM ANOVA, p_{time} <0.001, $p_{treatment}$ = 0.163, and $p_{timextreatment}$ = 0.134). On day 13 to day 20 post-L5Tx, all female mice that received i.t. injection regardless of the drug used (saline or CXCL1), showed significantly lower body weight than those mice that did not receive any injections (Figure 5B, two-way RM ANOVA, p_{time} < 0.001, $p_{treatment}$ = 0.041, and $p_{timextreatment}$ < 0.001).

When sensory sensitivity was examined, significant time and/or treatment-dependent sex effects were detected for both mechanical and heat sensitivity tests (three-way ANOVA, for von Frey test, p_{sex} < 0.001, $p_{sexxtime}$ = 0.022 and $p_{sexxtreatment}$ = 0.346; for the Hargreaves test, p_{sex} = 0.016, $p_{sexxtime}$ = 0.002 and $p_{sexxtreatment}$ = 0.004); therefore, all behavioral data were presented separately by sex (Figure 6). For mechanical sensitivity, both male and female mice displayed significant reduction of L5Tx-induced mechanical hypersensitivity during and shortly after the CXCL1 treatment. The lower dose of CXCL1 (1 ng/5 μl/injection) was determined to have a greater benefit compared to the higher dose of CXCL1 (10 ng/5 μl/injection) in both sexes (Figure 6A, two-way RM ANOVA, p_{time} < 0.001, $p_{treatment}$ = 0.005, and $p_{timextreatment}$ < 0.001, and Figure 6B, two-way RM ANOVA, p_{time} < 0.001, $p_{treatment}$ = 0.004, and $p_{timextreatment}$ = 0.001). However, the effective window for CXCL1 varied between sexes as peak effects for the lower dose of CXCL1 were seen between days 10 and 14 in males and between days 14 and 17 in females; and peak effects for the higher dose of CXCL1 were seen at day 10 in males and day 14 in females (Figures 6A and B). Further, there appeared to be a greater reduction in L5Tx-induced mechanical hypersensitivity in males than that in females following CXCL1 treatment. For heat sensitivity, CXCL1 treatment (regardless of the doses) did not significantly affect L5Tx-induced heat hypersensitivity in either male or female mice (Figure 6C, two-way RM ANOVA, p_{time} < 0.001, $p_{treatment}$ = 0.203, and $p_{timextreatment}$ = 0.643, and Figure 6D, two-way RM ANOVA, p_{time} < 0.001, $p_{treatment}$ = 0.396, and $p_{timextreatment}$ = 0.189), although there seemed to be a potential reduction in L5Tx-induced heat hypersensitivity in females, but not males, following the low dose CXCL1 treatment (Figure 6D, low dose CXCL1 at days 10–17; a quick sample size analysis indicated the minimal n = 100+ is needed to achieve statistical power of 0.8).

Lumbar spinal cord Ly6G expression post-L5Tx in both WT and CD40 KO mice

As CXCL1 is a potent neutrophil chemoattractant, we then examined the expression of neutrophil-specific gene, Ly6G in the lumbar spinal cord post-L5Tx in both WT and CD40 KO mice. As shown in Figure 7, L5Tx included increases of Ly6G expression in both WT and CD40 KO mice and the patterns of these increases are similar with the peak increase at day 7 post-L5Tx. However, the increase of Ly6G expression in CD40 KO mice is much higher than that in the WT mice (Figure 7, Two-way ANOVA, p_{time} < 0.001, $p_{animal\ group}$ < 0.001, and $p_{timexgroup}$ = 0.006).

Discussion

Following up on our previous findings regarding the contribution of CD4+ T cells and microglial CD40 in the maintenance of L5Tx-induced neuropathic pain, the current study investigated the roles of chemokines in CD4+ T cell-mediated and microglial CD40-mediated L5Tx-induced neuropathic pain-like behaviors by evaluating the RNA and protein levels of chemokines in the lumbar spinal cord following L5Tx in WT, CD4 KO, and CD40 KO mice. Due to the observed differential responses in CXCL1 expression as well as its corresponding receptor CXCR2 between WT, CD4 KO, and CD40 KO mice, we further examined the contribution of CXCL1 in L5Tx-induced behavioral hypersensitivity. Our results indicate a potential protective anti-nociceptive role of CXCL1. Further analysis on Ly6G expression suggests an associated increase of infiltrating neutrophils in the lumbar spinal cord post-L5Tx in CD40 KO mice.

CXCL1 (KC) is a well-known neutrophil attractant and within the CNS can be produced by microglia, astrocytes, and endothelial cells, as well as infiltrating neutrophils (Semple et al., 2010). The role of CXCL1 role in various chronic pain conditions has been investigated in recent years and contrary to our results, most studies to date have indicated a pro-nociceptive effect of CXCL1 (although there are obvious differences in the model systems used and genetic background of the study subjects). For example, Zhang et. al. reported a pro-nociceptive role of spinal cord CXCL1, mostly expressed by astrocytes, in a spinal nerve ligation model in outbred male ICR mice (Zhang et al., 2013). CXCL1 has also been shown to be involved in c-Jun N364 terminal kinase (JNK)-mediated sensory hypersensitivity in a rat model of cancer-induced bone pain (Wang et al., 2016). However, these studies did not examine the level of neutrophil infiltration in the spinal cord, thus did not link the effects of CXCL1 specifically to neutrophils. On the other hand, CXCL1 has also been investigated in various other disorders/conditions within the CNS, and some reports indicated a protective role for CXCL1. For example, CXCL1 injection induced an accumulation of neutrophils with an anti-inflammatory phenotype (N2 neutrophils) in a rat model of stroke (Easton, 2013). The mechanism through which CXCL1 mediates its anti-nociceptive effects (particularly mechanical hypersensitivity in our L5Tx model) requires further investigation. It is likely to be associated with increased infiltration of neutrophils due to the chemoattractant function of CXCL1, which is supported by our qRT-PCR data showing a greater increase of the expression of a neutrophil marker, Ly6G in the CD40 KO mice than in WT mice. However, due to the limited detection of infiltrating cells in lumbar spinal cords of CD40 KO mice following L5Tx (Cao et al., 2012a), we were not able to directly evaluate infiltrating neutrophils in our model system via flow cytometry. Neutrophil-specific immunohistochemistry may be needed in future studies. Besides exhibiting an anti-inflammatory function (N2-neutrophils) (Easton, 2013), neutrophils have been shown to produce opioid peptides that can lead to potent, clinically relevant, inhibition of pain in peripheral tissue following tissue damage (Machelska and Stein, 2006), and production of these peptides can be further investigated in the L5Tx model. In addition, the observed discrepancy in the effects of CXCL1 effects on L5Tx-induced mechanical vs. heat hypersensitivity further highlights the differential pathways involved in mechanical vs. heat

sensitivities as we have discussed extensively in a previous publication (Malon and Cao, 2016).

In our current study, we examined chemokine expression at both the protein and RNA levels. At the protein level (Figures 1 and 2), the most significant changes were seen in WT mice. Specifically, L5Tx induced significant upregulation of CCL2, CCL3, and CCL5 in WT but not CD4 KO mice. Although similar increases of these chemokines were observed in CD40 KO mice, the overall levels of these chemokines are much lower than that in WT mice; therefore, it is reasonable to propose that the lower levels of these pro-inflammatory chemokines following L5Tx contributes to the reduction of L5Tx-induced neuropathic pain behaviors in both CD4 KO and CD40 KO mice (Cao and DeLeo, 2008, Cao et al., 2009). Both CCL2 and CCL5 have been studied extensively regarding their pro-nociceptive roles in peripheral nerve injury-induced neuropathic pain development (Gao and Ji, 2010, Malon et al., 2011, Liou et al., 2012, Liou et al., 2013, Malon and Cao, 2016). Particularly, we have demonstrated that CD40 could contribute to L5Tx-inducemechanical hypersensitivity via both CGRP-independent/ CCL2 dependent, and CGRP/CCL5 -dependent pathways (Malon et al., 2011, Malon and Cao, 2016). CCL3 has also been implicated in the development of neuropathic pain-like behaviors in both peripheral nerve injury and chemotherapy induced neuropathic pain models (Kiguchi et al., 2010, Ochi-ishi et al., 2014, Sun et al., 2016). Our data also emphasized the notion that multiple chemokines, rather than one particularly chemokine, together promote the development and maintenance of peripheral nerve injury-induced neuropathic pain. Targeting only one chemokine may not provide the best treatment outcome. Interestingly, when we examined these chemokines at the transcript levels, knockout animals had comparable basal levels of these chemokines (in some cases higher levels than that in WT mice (Figure 3)), and L5Tx also induced significantly increased RNA levels of these chemokines in both CD4 KO (CCL2 and CCL5) and CD40 KO (CCL2, CCL3, and CCL5) mice (Figure 4) (particularly CD40 KO mice). These results suggest that CD4 T cells and microglial CD40 most likely mediate their respective pro-nociceptive roles by regulating spinal cord chemokine production at the protein (translational) level but not the transcriptional level. Nevertheless, comparable increases in RNA expression of these chemokines indicate the existence of compensatory regulations at the transcript level in both CD4 KO and CD40 KO mice. Moreover, comparing the expression of chemokines at the protein and RNA levels, it appears that global depletion of CD40 is associated with defects in chemokine protein production that cannot be rescued by increasing RNA expression either at basal level or following L5Tx.

Male and female mice were used in all experiments for this study. Unfortunately due to the low production of the knockout animals, especially CD4 KO mice, we cannot accurately evaluate the sex differences within our protein and RNA measurements. In the experiment involving CXCL1 treatment (Figures 5–6), we did observe statistical differences between males and females both in their body weight changes (Figure 5) and L5Tx-induced mechanical hypersensitivity (Figure 6) following CXCL1 treatment. Based on the body weight changes, it seems that females are more sensitive to i.t. injection procedure (including usage of isoflurane and injection itself) regardless of the solution being injected; while males are only sensitive to the higher dose of CXCL1 used. Further, male mice appeared to benefit from CXCL1 treatment sooner and more than female mice. It is well

established that neuropathic pain is more prevalent in females than males (Colloca et al., 2017). There is increasing evidence showing sex-dependent responses to peripheral nerve injury, and sex-dependent cellular/molecular mediators of neuropathic pain development in various mouse models of neuropathic pain (Sorge et al., 2011, Sorge et al., 2015, Vacca et al., 2016, Mapplebeck et al., 2017). Our results suggest the importance of further evaluating the effect s of CXCL1 in both sexes in the future studies, which could provide valuable guidance on designing respective treatment strategies for each sex.

Conclusions

Altogether, our results support previously published data on chemokines' pro-nociceptive role in neuropathic pain. However, more importantly our results suggested an anti-nociceptive role of CXCL1 in periphery nerve injury-induced neuropathic pain, which is potentially mediated by the infiltrating neutrophils. Further investigation into the underlying mechanisms of the protective function of CXCL1 may reveal novel drug targets for neuropathic pain treatment.

Acknowledgments

This work was supported by the National Institutes of Health [NIH/NIDA K01DA023503 (PI Cao), 2008–2012; NIH/NIGMS COBRE award, P20GM103643 (PD, Meng; sub-project PI, Cao), 2012–2016; NIH/NINDS R01NS098426 (PI Cao), 2016–2021). The funding agency had no role in study design, in the collection, analysis and interpretation of data, in the writing of the report, or in the decision to submit the article for publication. LC designed the study, performed animal surgeries, behavioral analysis and qRT-PCR assays, as well as drafted the manuscript. JTM performed animal surgeries and intrathecal injections, prepared samples for multiplex assays, and edited the manuscript.

References

Abbadie C, Lindia JA, Cumiskey AM, Peterson LB, Mudgett JS, Bayne EK, DeMartino JA, MacIntyre DE, Forrest MJ. Impaired neuropathic pain responses in mice lacking the chemokine receptor CCR2. Proc Natl Acad Sci U S A. 2003; 100:7947–7952. [PubMed: 12808141]

Callewaere C, Banisadr G, Rostene W, Parsadaniantz SM. Chemokines and chemokine receptors in the brain: implication in neuroendocrine regulation. J Mol Endocrinol. 2007; 38:355–363. [PubMed: 17339398]

Cao L, Beaulac H, Eurich A. Differential lumbar spinal cord responses among wild type, CD4 knockout, and CD40 knockout mice in spinal nerve L5 transection-induced neuropathic pain. Molecular Pain. 2012a; 8:88–88. [PubMed: 23249743]

Cao L, Butler MB, Tan L, Draleau KS, Koh WY. Murine immunodeficiency virus-induced peripheral neuropathy and the associated cytokine responses. J Immunol. 2012b; 189:3724–3733. [PubMed: 22956581]

Cao L, DeLeo JA. CNS-infiltrating CD4+ T lymphocytes contribute to murine spinal nerve transection-induced neuropathic pain. Eur J Immunol. 2008; 38:448–458. [PubMed: 18196515]

Cao L, Palmer CD, Malon JT, De Leo JA. Critical role of microglial CD40 in the maintenance of mechanical hypersensitivity in a murine model of neuropathic pain. Eur J Immunol. 2009; 39:3562–3569. [PubMed: 19750482]

Chaplan SR, Bach FW, Pogrel JW, Chung JM, Yaksh TL. Quantitative assessment of tactile allodynia in the rat paw. J Neurosci Methods. 1994; 53:55–63. [PubMed: 7990513]

Charo IF, Ransohoff RM. The many roles of chemokines and chemokine receptors in inflammation. N Engl J Med. 2006; 354:610–621. [PubMed: 16467548]

Christophi GP, Hudson CA, Panos M, Gruber RC, Massa PT. Modulation of macrophage infiltration and inflammatory activity by the phosphatase SHP-1 in virus-induced demyelinating disease. J Virol. 2009; 83:522–539. [PubMed: 18987138]

Clark AK, Malcangio M. Fractalkine/CX3CR1 signaling during neuropathic pain. Front Cell Neurosci. 2014; 8:121. [PubMed: 24847207]

Colloca L, Ludman T, Bouhassira D, Baron R, Dickenson AH, Yarnitsky D, Freeman R, Truini A, Attal N, Finnerup NB, Eccleston C, Kalso E, Bennett DL, Dworkin RH, Raja SN. Neuropathic pain. Nature reviews Disease primers. 2017; 3:17002–17002.

Draleau KS, Maddula S, Slaiby A, Nutile-McMenemy N, De Leo JA, Cao L. Phenotypic Identification of Spinal Cord-Infiltrating CD4(+) T Lymphocytes in a Murine Model of Neuropathic Pain. Journal of pain & relief. 2014; (Suppl 3):003. [PubMed: 25143871]

Easton AS. Neutrophils and stroke – can neutrophils mitigate disease in the central nervous system? International Immunopharmacology. 2013; 17:1218–1225. [PubMed: 23827753]

Fleming TJ, Fleming ML, Malek TR. Selective expression of Ly-6G on myeloid lineage cells in mouse bone marrow. RB6-8C5 mAb to granulocyte-differentiation antigen Gr-1) detects members of the Ly-6 family. The Journal of Immunology. 1993; 151:2399–2408. [PubMed: 8360469]

Gao YJ, Ji RR. Chemokines, neuronal-glial interactions, and central processing of neuropathic pain. Pharmacol Ther. 2010; 126:56–68. [PubMed: 20117131]

Gao YJ, Zhang L, Samad OA, Suter MR, Yasuhiko K, Xu ZZ, Park JY, Lind AL, Ma Q, Ji RR. JNK-induced MCP-1 production in spinal cord astrocytes contributes to central sensitization and neuropathic pain. J Neurosci. 2009; 29:4096–4108. [PubMed: 19339605]

Gaskin DJ, Richard P. The economic costs of pain in the United States. J Pain. 2012; 13:715–724. [PubMed: 22607834]

Jensen TS, Baron R, Haanpää M, Kalso E, Loeser JD, Rice ASC, Treede R-D. A new definition of neuropathic pain. Pain. 2011; 152:2204–2205. [PubMed: 21764514]

Kiguchi N, Kobayashi Y, Maeda T, Saika F, Kishioka S. CC-chemokine MIP-1Î± in the spinal cord contributes to nerve injury-induced neuropathic pain. Neuroscience Letters. 2010; 484:17–21. [PubMed: 20692319]

Liou JT, Mao CC, Ching-Wah Sum D, Liu FC, Lai YS, Li JC, Day YJ. Peritoneal administration of Met-RANTES attenuates inflammatory and nociceptive responses in a murine neuropathic pain model. J Pain. 2013; 14:24–35. [PubMed: 23183003]

Liou JT, Yuan HB, Mao CC, Lai YS, Day YJ. Absence of C-C motif chemokine ligand 5 in mice leads to decreased local macrophage recruitment and behavioral hypersensitivity in a murine neuropathic pain model. Pain. 2012; 153:1283–1291. [PubMed: 22494919]

Machelska H, Stein C. Leukocyte-Derived Opioid Peptides and Inhibition of Pain. Journal of Neuroimmune Pharmacology. 2006; 1:90–97. [PubMed: 18040794]

Malon JT, Cao L. Calcitonin gene-related peptide contributes to peripheral nerve injury-induced mechanical hypersensitivity through CCL5 and p38 pathways. Journal of Neuroimmunology. 2016; 297:68–75. [PubMed: 27397078]

Malon JT, Maddula S, Bell H, Cao L. Involvement of calcitonin gene-related peptide and CCL2 production in CD40-mediated behavioral hypersensitivity in a model of neuropathic pain. Neuron Glia Biol. 2011; 7:117–128. [PubMed: 22377050]

Mapplebeck JCS, Beggs S, Salter MW. Molecules in pain and sex: a developing story. Molecular Brain. 2017; 10:9. [PubMed: 28270169]

Ochi-ishi R, Nagata K, Inoue T, Tozaki-Saitoh H, Tsuda M, Inoue K. Involvement of the chemokine CCL3 and the purinoceptor P2X7 in the spinal cord in paclitaxel-induced mechanical allodynia. Molecular Pain. 2014; 10:53–53. [PubMed: 25127716]

Semple BD, Kossmann T, Morganti-Kossmann MC. Role of chemokines in CNS health and pathology: a focus on the CCL2/CCR2 and CXCL8/CXCR2 networks. Journal of Cerebral Blood Flow and Metabolism: Official Journal of the International Society of Cerebral Blood Flow and Metabolism. 2010; 30:459–473.

Sorge RE, LaCroix-Fralish ML, Tuttle AH, Sotocinal SG, Austin J-S, Ritchie J, Chanda ML, Graham AC, Topham L, Beggs S, Salter MW, Mogil JS. Spinal cord Toll-like receptor 4 mediates inflammatory and neuropathic hypersensitivity in male but not female mice. The Journal of

neuroscience : the official journal of the Society for Neuroscience. 2011; 31:15450–15454. [PubMed: 22031891]

Sorge RE, Mapplebeck JCS, Rosen S, Beggs S, Taves S, Alexander JK, Martin LJ, Austin J-S, Sotocinal SG, Chen D, Yang M, Shi XQ, Huang H, Pillon NJ, Bilan PJ, Tu YS, Klip A, Ji R-R, Zhang J, Salter MW, Mogil JS. Different immune cells mediate mechanical pain hypersensitivity in male and female mice. Nature neuroscience. 2015; 18:1081–1083. [PubMed: 26120961]

Sun S, Chen D, Lin F, Chen M, Yu H, Hou L, Li C. Role of interleukin-4, the chemokine CCL3 and its receptor CCR5 in neuropathic pain. Molecular Immunology. 2016; 77:184–192. [PubMed: 27522478]

Vacca V, Marinelli S, Pieroni L, Urbani A, Luvisetto S, Pavone F. 17beta-estradiol counteracts neuropathic pain: a behavioural, immunohistochemical, and proteomic investigation on sex-related differences in mice. Scientific Reports. 2016; 6:18980. [PubMed: 26742647]

Wang, Z-l, Du, T-t, Zhang, R-g. JNK in spinal cord facilitates bone cancer pain in rats through modulation of CXCL1. Journal of Huazhong University of Science and Technology [Medical Sciences]. 2016; 36:88–94.

White FA, Jung H, Miller RJ. Chemokines and the pathophysiology of neuropathic pain. Proc Natl Acad Sci U S A. 2007; 104:20151–20158. [PubMed: 18083844]

Zhang ZJ, Cao DL, Zhang X, Ji RR, Gao YJ. Chemokine contribution to neuropathic pain: respective induction of CXCL1 and CXCR2 in spinal cord astrocytes and neurons. Pain. 2013; 154:2185–2197. [PubMed: 23831863]

Highlights

1. L5Tx induced significantly reduced chemokine responses in both CD4 KO and CD40 KO mice.
2. L5Tx induced a significant increase in CXCL1 expression at the protein level in CD40 KO mice but not WT or CD4 KO mice.
3. Administration of CXCL1 reduced L5Tx-induced mechanical hypersensitivity in WT mice.
4. CD40 KO mice expressed significantly higher levels of Ly6G than WT mice in the lumbar spinal cord post-L5Tx.

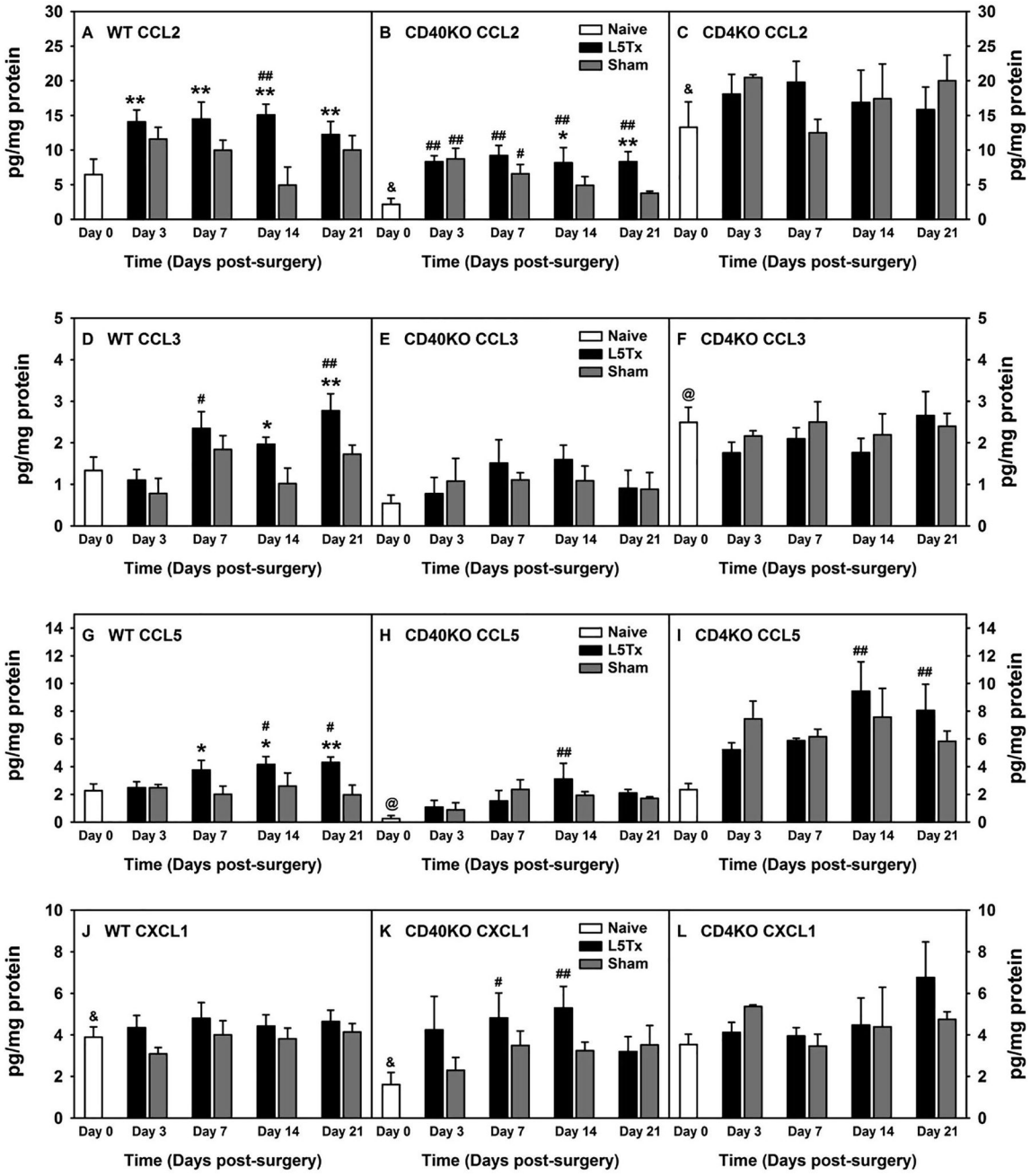

Figure 1. Lumbar spinal cord chemokine expression at the protein level (absolute levels) following L5Tx in WT, CD40 KO, and CD4 KO mice

WT BALB/c (A, D, G and J), CD40 KO (B, E, H, and K), and CD4 KO (C, F, I and L) mice were randomly assigned to naïve, L5Tx, or sham groups. Lumbar spinal cords were collected before surgery (naïve; i.e. “Day 0” in the graph), and days 3, 7, 14, and 21 after surgery. Chemokines: CXCL1 (KC), CCL1 (TCA-3), CCL2 (MCP-1), CCL3 (MIP-1α), CCL5 (RANTES), CCL11 (eotaxin), CCL17 (TARC), and CCL22 (MDC) within spinal cord samples were determined via a multiplex assay by Quansys Biosciences. Data for chemokines, CCL2 (A–C), CCL3 (D–F), CCL5 (G–I), and CXCL1 (J–L) are presented as mean ± SEM (WT n = 6–10, CD40 KO n = 6 and CD4 KO n = 3). & $p < 0.05$ between

indicated naïve groups for the same chemokine; @ $p < 0.05$ compared to naïve groups from all other genotype of mice for the same chemokine; # $p < 0.1$ and ## $p < 0.05$ compared to corresponding naïve group; and * $p < 0.1$ and ** $p < 0.05$ compared to corresponding sham group.

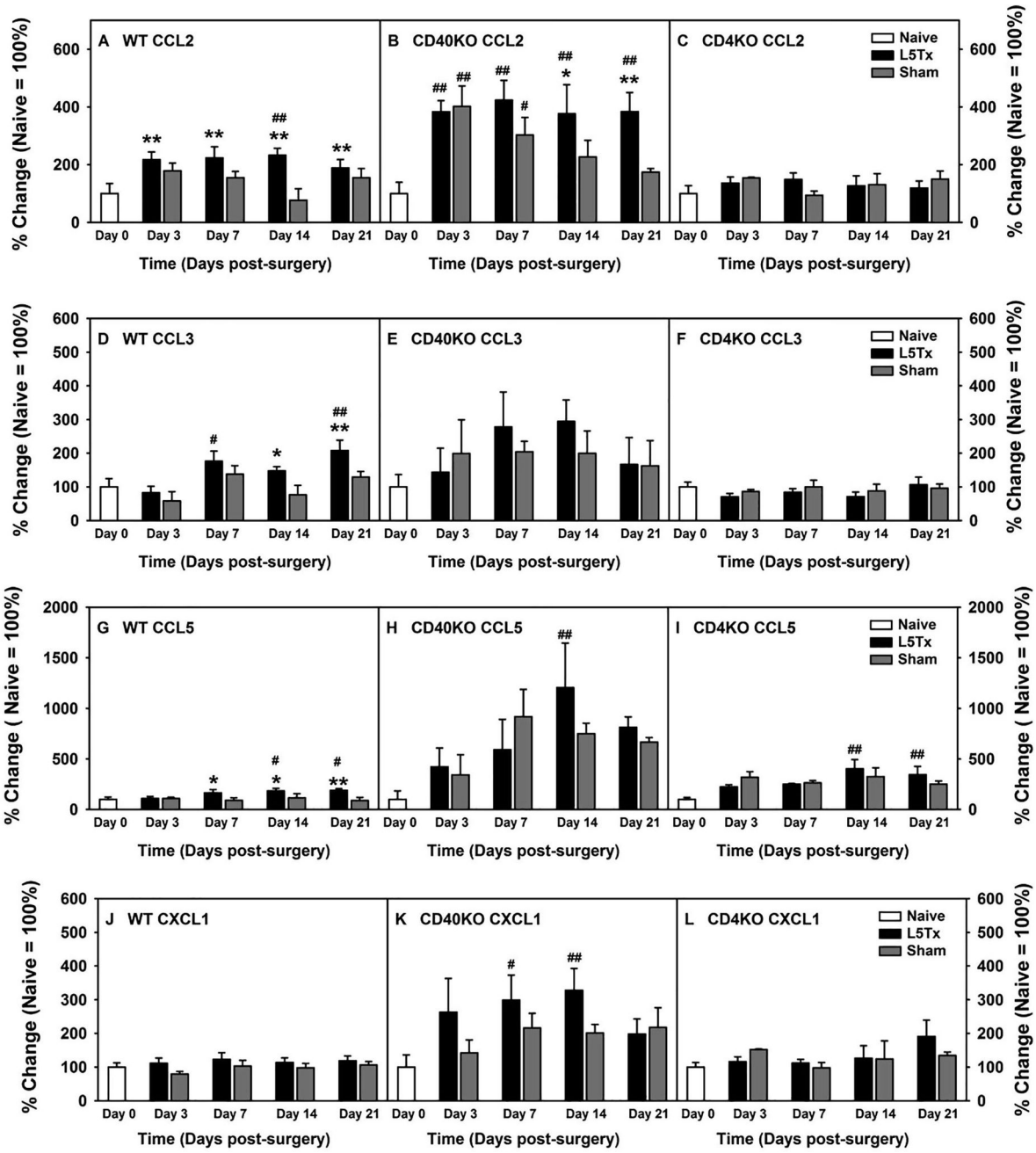

Figure 2. Lumbar spinal cord chemokine expression at the protein level (percentage changes) following L5Tx in WT, CD40 KO, and CD4 KO mice

Data were obtained as described in Figure 1. Due to significant differences at the basal levels of the chemokines shown in Figure 1, percentage change of each chemokine following each surgery within each genotype of mice were calculated (naive = 100% within each genotype) and presented here. All letter labels (A–L) used in Figure 2 are the same as that in Figure 1. Data are presented as mean ± SEM (WT n = 6–10, CD40 KO n = 6 and CD4 KO n = 3). & $p < 0.05$ between indicated naïve groups for the same chemokine; @ $p < 0.05$ compared to naïve groups from all other genotype of mice for the same chemokine; # $p < 0.1$ and ## $p <$

0.05 compared to corresponding naïve group; and * $p < 0.1$ and ** $p < 0.05$ compared to corresponding sham group. “Day 0” = naive.

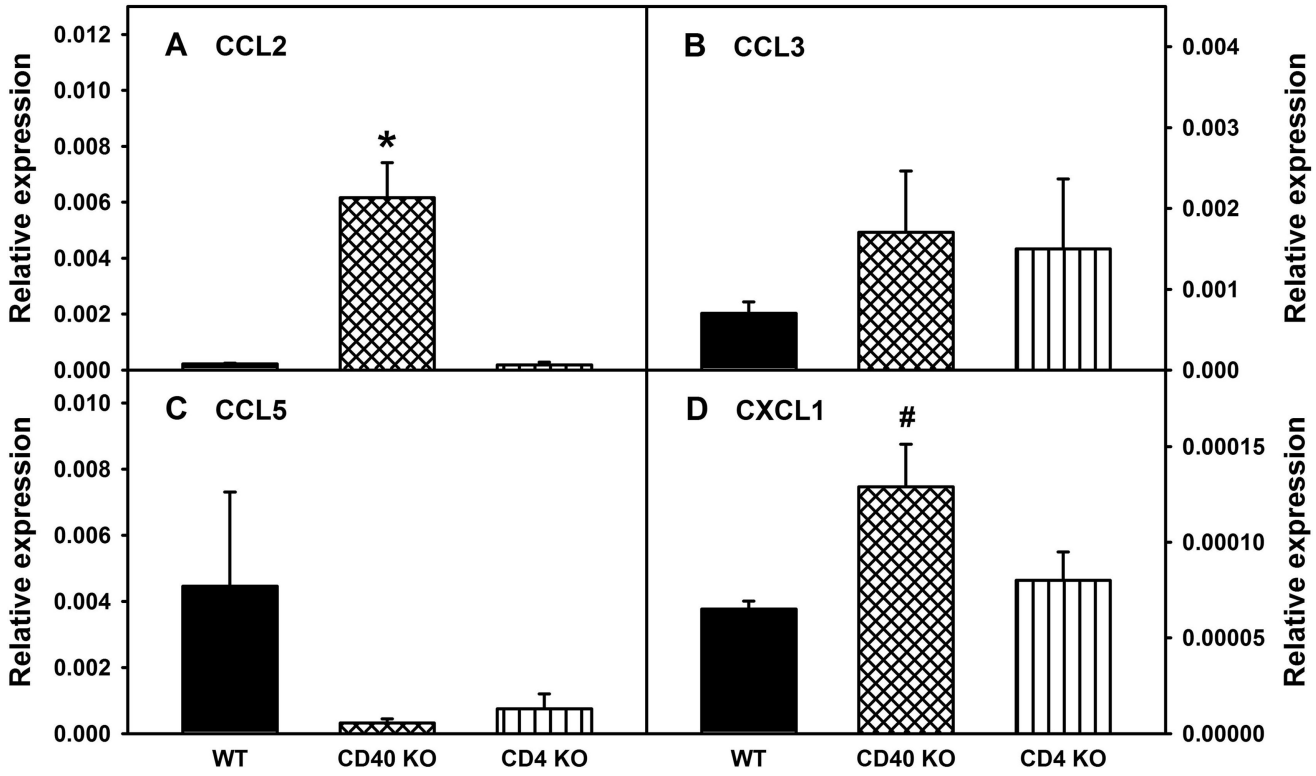

Figure 3. RNA expression of selected chemokines in the lumbar spinal cord at basal levels in WT, CD40 KO, and CD4 KO mice

Lumbar spinal cords were collected from naïve WT BALB/c, CD40 KO, and CD4 KO mice and the RNA expression of chemokines, CCL2 (A), CCL3 (B), CCL5 (C), and CXCL1 (D) in the lumbar spinal cords were determined via real-time qRT-PCR using GAPDH as control. Data are presented as mean ± SEM (n = 4 for all). * $p < 0.05$ compared to all other genotypes of mice, and # $p < 0.05$ compared to WT mice.

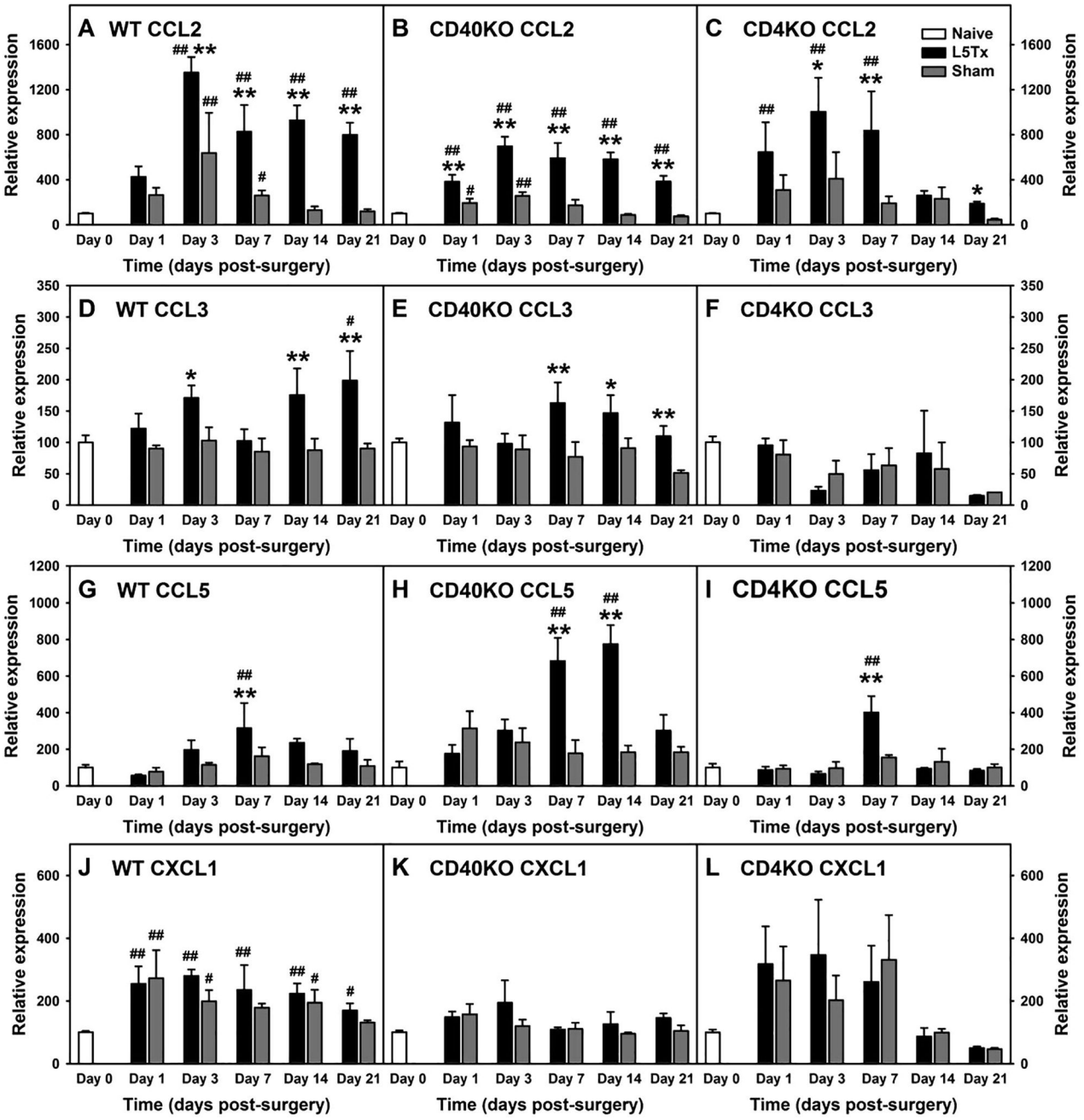

Figure 4. Lumbar spinal cord chemokine RNA expression following L5Tx in WT, CD40 KO and CD4 KO mice

WT BALB/c (A, D, G and J), CD40 KO (B, E, H, and K) and CD4 KO (C, F, I and L) mice were randomly assigned to either L5Tx or sham groups. Lumbar spinal cords were collected before surgery (naïve; i.e. "Day 0" in the graph), and days 1, 3, 7, 14, and 21 after surgery. RNA expression of chemokines, CCL2 (A–C), CCL3 (D–F), CCL5 (G–I), and CXCL1 (J–L) within these spinal cord samples were determined via real-time qRT-PCR using GAPDH as control. Percentage changes of each chemokines following surgeries within each genotype of mice (naive = 100%) were calculated and presented here. Data are presented as mean ± SEM (WT n = 4, CD40 KO n = 4, and CD4 KO n = 2–4). # $p < 0.1$ and ## $p < 0.05$

compared to corresponding naïve group; and * $p < 0.1$, and ** $p < 0.05$ compared to corresponding sham group.

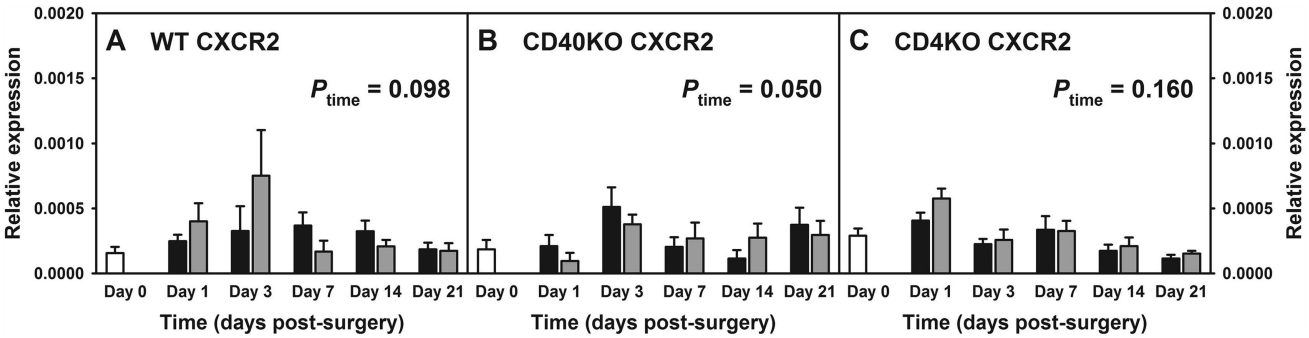

Figure 5. Lumbar spinal cord CXCR2 RNA expression following L5Tx in WT, CD40 KO and CD4 KO mice

Lumbar spinal cord samples from WT BALB/c (A), CD40 KO (B) and CD4 KO (C) mice as described in Figure 4 were used. RNA expression of chemokine receptor CXCR2 within these spinal cord samples were determined via real-time qRT-PCR using GAPDH as control. Data are presented as mean ± SEM (WT n = 4, CD40 KO n = 4, and CD4 KO n = 2–4). P value within each graph indicates the time effect detected by two-way ANOVA. Day 0 = Naïve.

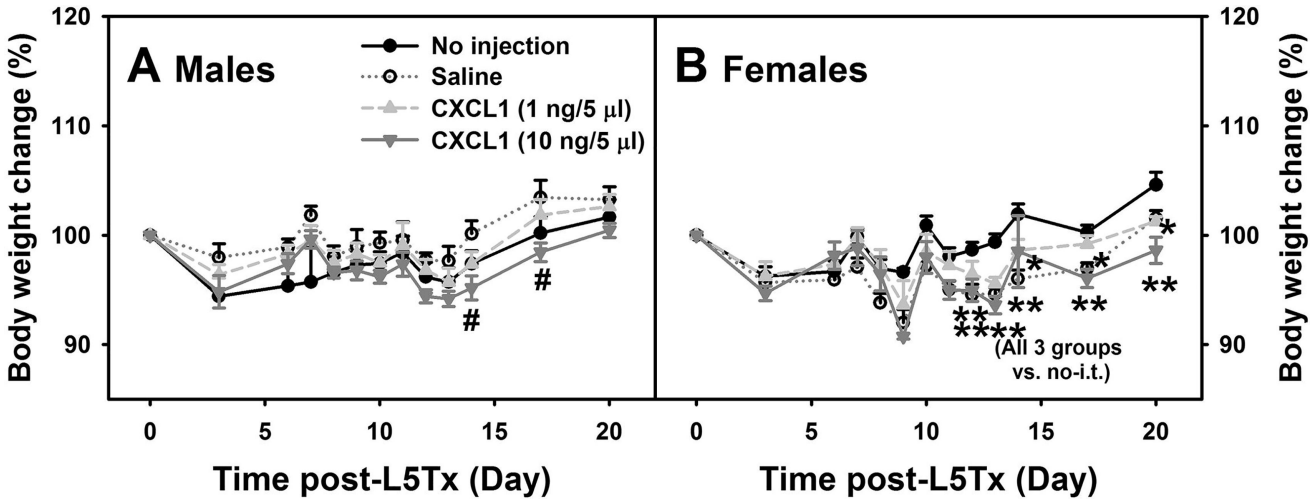

Figure 6. Effects of CXCL1 on body weight changes following L5Tx in WT mice

WT mice were randomly divided into the following 4 treatment groups: no i.t. injection, saline i.t. injection, and recombinant mouse CXCL1 (at 1 ng/5 µl/mouse or 10 ng/5 µl/mouse) i.t. injections. Injections were given daily from day 6–13 post-L5Tx. Body weight of all animals were monitored from before the initiation of the experiment (baselines) until the end of the experiment, day 20 post-L5Tx. Data are shown in males (A) and females (B) separately due to that the initial statistical analysis suggested sex differences (mean ± SEM, n = 6). # $p < 0.05$ between the saline group and the high dose CXCL1 (10 ng /5 µl) group, and ** $p < 0.05$, * $p < 0.1$ compared to "no injection" group.

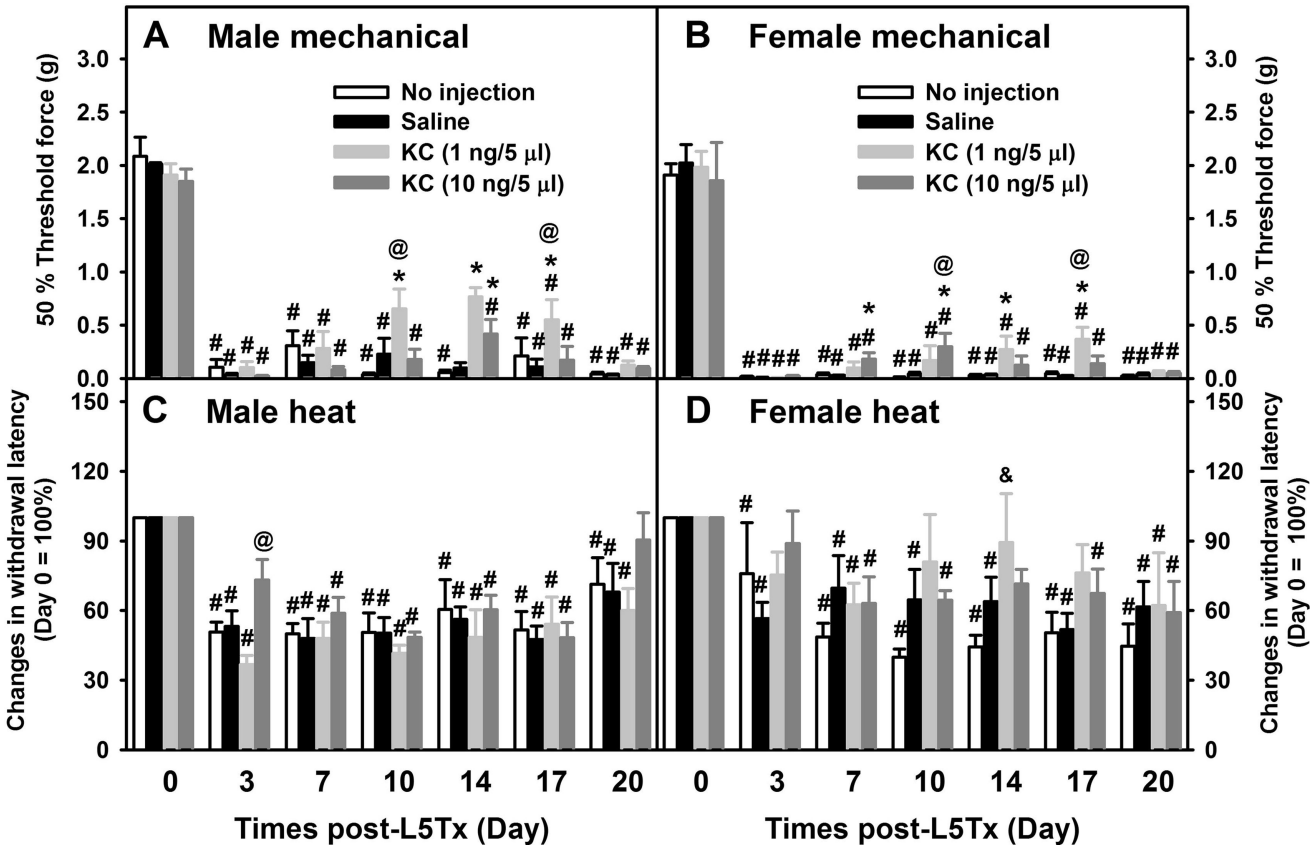

Figure 7. Effects of CXCL1 on L5Tx-induced mechanical and heat hypersensitivities in WT mice

Mechanical (A and B) and heat (C and D) sensitivities were measured in WT mice (same mice described in Figure 5 legend) that received no i.t. injection, saline i.t. injection, or recombinant mouse CXCL1 (at 1 ng/5 μl/mouse or 10 ng/5 μl/mouse) i.t. injections daily from day 6–13 post-L5Tx. Mechanical (A and B) and heat (C and D) sensitivities were measured via the up-down method and the Hargreaves test respectively. Data are shown in males (A and C) and females (B and D) separately due to that the initial statistical analysis suggested sex differences (mean ± SEM, n = 6). # $p < 0.05$ compared to corresponding naïve group (Day 0). * $p < 0.05$ compared to both “no injection” and ”saline” groups at the same time point, & $p < 0.05$ compared to “no injection” group at the same time point, and & $p < 0.05$ between the low dose (1 ng/5 μl) and high dose (10 ng/5 μl) CXCL1 treatment groups at the same time point.

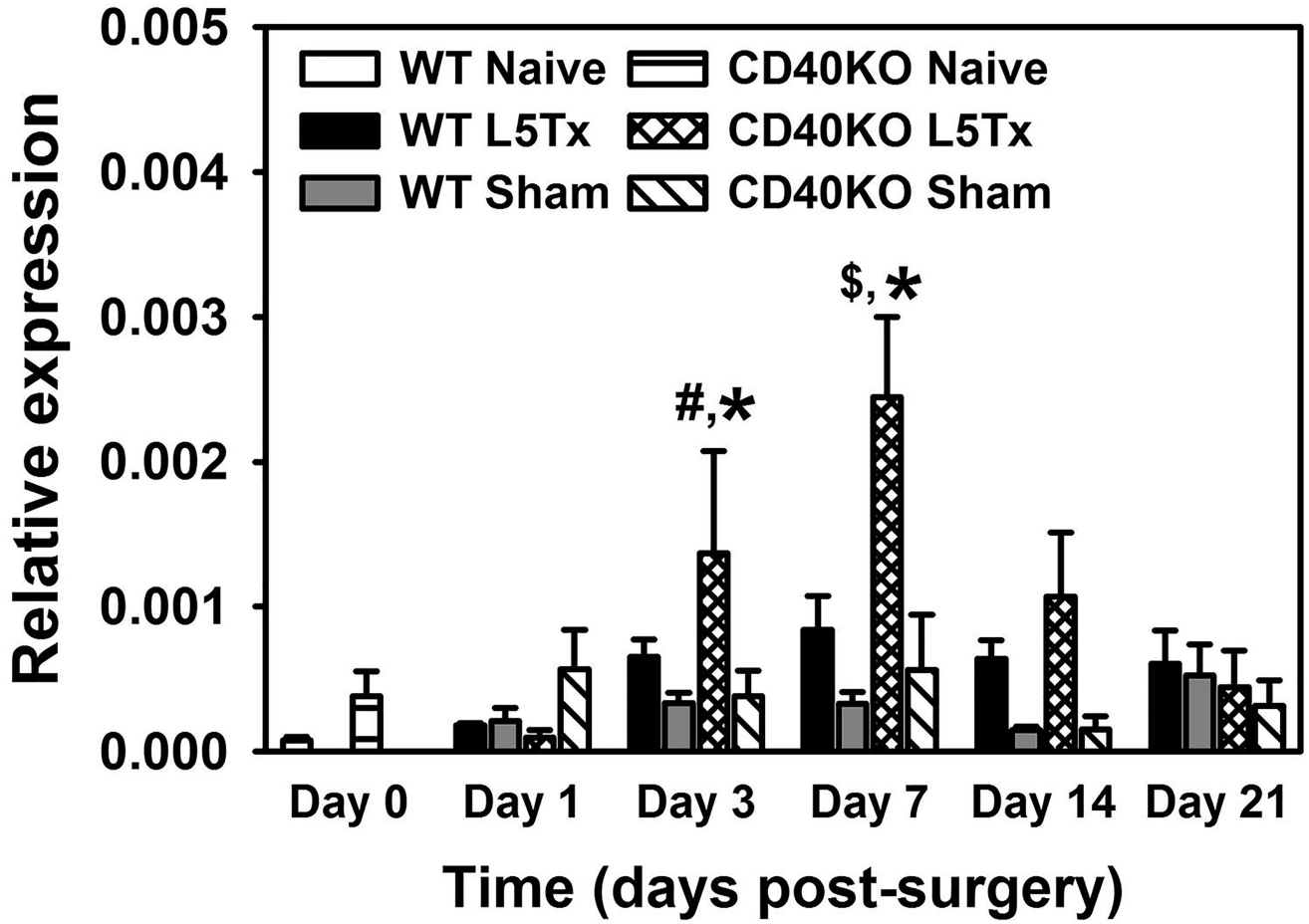

Figure 8. RNA expression of Ly6G in the lumbar spinal cord post-L5Tx in WT and CD40 KO mice

Lumbar spinal cords were collected before surgery (naïve; i.e. "Day 0" in the graph), and days 1, 3, 7, 14, and 21 after surgery. RNA expression of Ly6G within these spinal cord samples were determined via real-time qRT-PCR using GAPDH as control. Data are presented as mean ± SEM (n = 4). * $p < 0.05$ compared to all other groups at the same time point, # $p < 0.05$ compared to corresponding naïve and "Day 1" groups, and $ $p < 0.05$ compared to all other "L5Tx" groups within the same genotype.

Table-1

Summary of primer sequences used for qRT-PCR.

Target Gene	Forward Primer (5′-3′)	Reverse Primer (5′-3′)	Sources
CXCL1	GTGCCATCAGAGCAGTCT	CCAAACCGAAGTCATAGCCA	IDT PrimeTime
CXCR2	GCCTCACTTTCTTCCAGTTCA	ATCCACCTTGAATTCTCCCATC	IDT PrimeTime
Ly6G	TTGACAGCATTACCAGTGATCT	GCGTTGCTCTGGAGATAGAAG	IDT PrimeTime
GAPDH	GTGGAGTCATACTGGAACATGTAG	AATGGTGAAGGTCGGTGTG	IDT PrimeTime
CCL2	GTATGTCTGGACCCATTCCTTC	GCTGTAGTTTTTGTCACCAAGC	Christophi et al., 2009 (Christophi et al., 2009)
CCL3	CAGCCAGGTGTCATTTTCCT	AGGCATTCAGTTCCAGGTCA	Christophi et al., 2009 (Christophi et al., 2009)
CCL5	AGCTGCCCTCACCATCATC	CTCTGGGTTGGCACACACTT	Christophi et al., 2009 (Christophi et al., 2009)
GAPDH	ACCACCATGGAGAAGGC	GGCATGGACTGTGGTCATGA	Christophi et al., 2009 (Christophi et al., 2009)